

Low Energy Monopropellants Based on the Guanylurea Cation

Thomas M. Klapötke*^[a] and Carlos Miró Sabaté^[a]

Keywords: Guanylurea; Energetic materials; X-ray diffraction; Density functional calculations; NMR spectroscopy

Abstract. Reaction of cyanoguanidine (**3**) with hydrochloric, sulfuric, nitric or perchloric acids yielded guanylurea chloride (**4**), sulfate (**5**), nitrate (**6**) and perchlorate (**7**). Compounds **4** and **5** reacted further to form a new family of energetic salts based on the guanylurea cation and azide (**8a**), 5-nitrotetrazolate (**9**), 5-aminotetrazolate (**10**), picrate (**11**) and 5,5'-azotetrazolate (**12a**) anions. The water of hydration in compounds **8a** and **12a** was eliminated by heating under vacuum yielding the anhydrous salts **8b** and **12b**. All materials were characterized by means of elemental analysis, mass spectrometry (MS) as well as vibrational (IR, Raman) and NMR (¹H, ¹³C, ^{14/15}N and ³⁵Cl) spectroscopy. Additionally, the crystal structures of **4**, **7**, **8a** and **10** were determined by low temperature X-ray measurements (**4**, **7** and **8a**: Monoclinic, *P2₁/c*; **10**: Monoclinic, *P2₁*). The thermal behavior of **6**–**12** was assessed by DSC measurements and their heats of formation were cal-

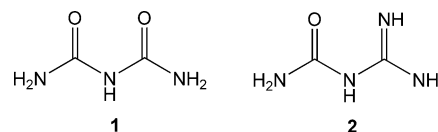
culated on the basis of the electronic energies of the ions using the MP2 method. In addition, the sensitivity to shock, friction and electrostatic discharge of all materials was measured by submitting the compounds to standard (BAM) tests. The detonation pressures (*P*) and velocities (*D*) were calculated from the energies of formation using the EXPLO5 code (**6**: *P* = 17.4 GPa, *D* = 7004 m·s⁻¹; **8a**: *P* = 20.6 GPa, *D* = 7880 m·s⁻¹; **8b**: *P* = 16.9 GPa, *D* = 7289 m·s⁻¹; **9**: *P* = 20.3 GPa, *D* = 7439 m·s⁻¹; **10**: *P* = 18.4 GPa, *D* = 7530 m·s⁻¹; **11**: *P* = 19.7 GPa, *D* = 7152 m·s⁻¹; **12a**: *P* = 24.3 GPa, *D* = 8222 m·s⁻¹ and **7**: *P* = 23.3 GPa, *D* = 8115 m·s⁻¹). Lastly, the long term stability of **12a** was assessed and the ICT code was used to predict the decomposition gases. Most materials decompose giving large amount of environmentally friendly gases and their performance values classify them as new insensitive low-energy monopropellants.

Introduction

The synthesis of energetic materials has been a topic of considerable interest especially over the last years [1]. Much work has been devoted towards the synthesis ofazole-based energetic salts [1f–l, 2] and the scanning of different combinations of anions and cations [3]. The impact on properties of new energetic compounds in view of the different cations and anions provides substantial knowledge. For example, combination with ions with high nitrogen contents results in endothermic (or little exothermic) compounds, whereas well oxygen balanced compounds have often the best performance or for example, dinitramide salts have generally lower melting points and thermal stabilities than analogous nitrate salts.

In the recent past, we reported on new neutral energetic materials based on biuret (**1**) [4], which have adequate performance values, however as observed for urea, energetic compounds based on **1** are relatively labile (e.g., dinitrobiuret decomposes in protic solvents). Different studies gave credit for the higher stability of salts with guanidinium cations (i.e., guanidinium, amino-, diamino- and triaminoguanidinium) in

respect to urea-based compounds. In this context, the parent **2** (guanylurea, GU), which can be seen as the monoimine of **1**, should have a better stability because of the guanidine moiety (see Scheme 1). Although salts of **2** were already reported as early as 1933 [5], a synthesis for the free acid (**2**) did not appear until 1942 [6]. Complexes of **2** were reported to have fungicide [7] and antitumor (i.e., with Pt) [8] properties and recently there has been considerable interest in the use of **2** as a bidentate ligand for coordination chemistry [9] although alkylated derivatives had already been used before [10]. Guanidines have also attracted people's interest for the synthesis of energetic materials [11] and guanylurea dinitramide (FOX-12) has recently been described in several patents [12] as a new promising energetic compound for low-sensitivity munitions in propellants and explosives applications. The compound can be conveniently synthesized by a metathesis reaction of commercially available guanylurea sulfate (**5**) with ammonium dinitramide in high yield [13]. However, a cheap source of the dinitramide anion (–N(NO₂)₂) is not available in the open literature, which makes the production of FOX-12 rather expensive.



Scheme 1. Structural formulas of biuret (**1**) and guanylurea (**2**).

The formal replacement of one of the oxygen atoms in **1** by an amino group in the salts of **2** should allow for the formation

* Prof. Dr. T. M. Klapötke
Fax: +49-89-2180-77492
E-Mail: tmk@cup.uni-muenchen.de

[a] Department of Chemistry and Biochemistry Energetic Materials Research
Ludwig-Maximilian University
Butenandstr. 5–13
81377 Munich., Germany

Supporting information for this article is available on the WWW under <http://dx.doi.org/10.1002/zaac.200900330> or from the author.

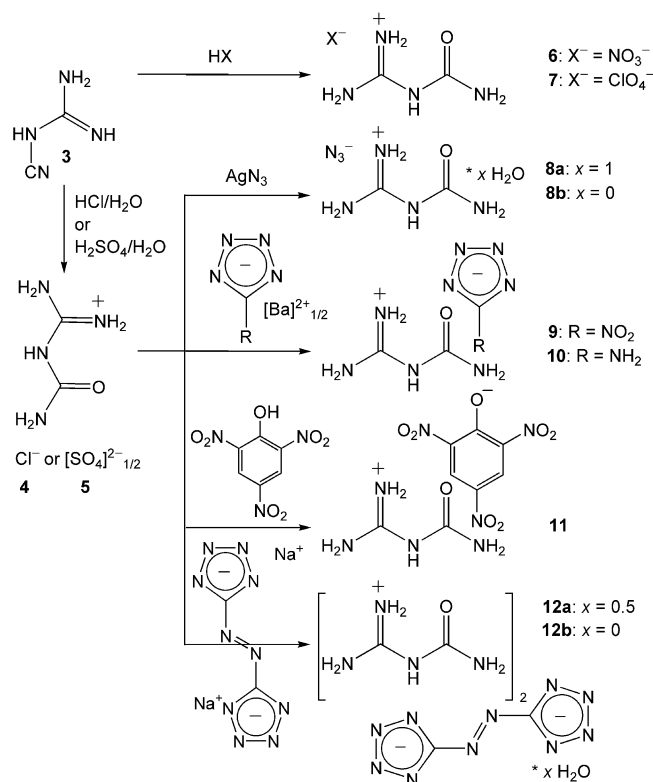
of extensive hydrogen-bonding networks in the solid state. Such networks help to stabilize the material considerably and are, for example, responsible for the low sensitivity of 1,1-amino-2,2-dinitroethene (FOX-7) [14]. Ionic energetic materials based on guanidines are also known to form strong hydrogen-bonding networks and can show remarkable stability and considerable insensitivity to physical stimuli. Salts such as ammonium nitrate (AN), perchlorate (AP) and dinitramide (ADN) are commonly used as oxidizers in explosive and currently used propellant mixtures to compensate for the negative oxygen balances and boost the performance. In addition, ionic energetic materials tend to exhibit lower vapor pressure (essentially eliminating the risk of exposure through inhalation) than similar neutral non-ionic analogues [15].

Surprisingly, regardless of the potential of guanylurea chloride monohydrate [16] and guanylurea sulfate (5) as starting materials for the synthesis of energetic compounds and the interesting energetic properties of the dinitramide salt, the latter remains as the only report of a guanylurea salt, which has been considered for energetic applications. The nitrate salt (6) had been either only mentioned [17] or described in the non-international literature [18] prior to our studies [19]. Thus, we decided to investigate the potential of the GU^+ cation to form energetic salts in combination with highly endothermic anions (N_3^- , $[\text{N}_4\text{C}-\text{NO}_2]^-$, $[\text{N}_4\text{C}-\text{NH}_2]^-$ and $[\text{N}_4\text{C}-\text{N}=\text{N}-\text{CN}_4]^{2-}$) and oxygen-rich anions ($[\text{N}_4\text{C}-\text{NO}_2]^-$ and picrate). The detonation parameters of the new compounds as well as those of formulations with an oxidizer (AN and ADN) were calculated. Lastly, due to the increasing environmental concern the gases formed upon decomposition of the compounds were predicted using a computer code.

Results and Discussion

Synthesis

In order to synthesize the guanylurea cation (GU^+), cyanoguanidine (3) was hydrolyzed and protonated with a strong acid (i.e., hydrochloric or sulfuric acid) to form guanylurea chloride (4) or guanylurea sulfate (5), as indicated in Scheme 2. Alternatively, other strong acids such as nitric acid or perchloric acid could also be used rendering the energetically interesting nitrate (6) and perchlorate (7) salts. Metathesis reactions of 4 with a silver or sodium salt, led to the formation of the azide (8a) and 5,5'-azotetrazolate (12a) salts, which formed as the hydrated species. The water of crystallization could be conveniently removed by heating the compounds under vacuum rendering the anhydrous materials (8b and 12b). On the other hand, reaction of the sulfate salt (5) with a suitable barium tetrazolate salt, allowed us to isolate the 5-nitrotetrazolate (9) and 5-aminotetrazolate (10) salts, after separating the precipitated barium sulfate. Because of the high insolubility of the picrate salt (11), this could be prepared by direct reaction between the chloride salt (4) and picric acid. All materials were characterized by means of elemental analysis, mass spectrometry (MS) and vibrational (IR, Raman) and NMR (^1H , ^{13}C and/or ^{14}N NMR) spectroscopy. Additionally, the crystal structures of 4, 7, 8a and 10 were determined.



Scheme 2. Synthesis of guanylurea salts 4–12.

Lastly, compounds 4–10 were isolated as colorless powders, which are readily soluble in water and other polar solvents such as DMSO, DMF or short chain alcohols, whereas salts 11, 12a and 12b are only slightly soluble in boiling water, moderately soluble in DMSO or DMF and completely insoluble in any other common solvent.

Vibrational and NMR Spectroscopy

All quantum chemical calculations (see also “Thermal and Energetic Properties” section) were carried out with the Gaussian03W software package [20]. Vibrational (IR and Raman) frequencies of the guanylurea cation were calculated using Becke's B3 three parameter hybrid function with an LYP correlation function (B3LYP)[21] and were scaled by a factor of 0.9614 as described by Radom et al. [22]. For all atoms in all calculations, the correlation consistent polarized double-zeta basis set cc-pVDZ was used [23, 24].

All salts were qualitatively identified by IR and Raman spectroscopy. The bands of the corresponding anions can be easily identified by their characteristic fingerprints. In the Raman spectra, they are found at 1054 cm^{-1} (NO_3^- , 6), 932 and 461 cm^{-1} (ClO_4^- , 7), $\approx 1340\text{ cm}^{-1}$ (N_3^- , 8a and 8b), 1422 , 1064 and 1032 cm^{-1} ($[\text{N}_4\text{C}-\text{NO}_2]^-$, 9), 1714 cm^{-1} ($[\text{N}_4\text{C}-\text{NH}_2]^-$, 10), 1316 cm^{-1} ($[(\text{NO}_2)_3\text{Ph}-\text{O}]^-$, 11) and at ≈ 1480 and 1380 cm^{-1} ($[\text{N}_4\text{C}-\text{N}=\text{N}-\text{CN}_4]^{2-}$, 12a and 12b). The stretches of the anions are, as expected, of lower intensity in the IR spectra and observed at 1385 cm^{-1} (NO_3^- , 6), 1089 cm^{-1} (ClO_4^- , 7),

$\approx 2040 \text{ cm}^{-1}$ (N_3^- , **8a** and **8b**), 1420 , 1060 and 1022 cm^{-1} ($[\text{N}_4\text{C}-\text{NO}_2]^-$, **9**), 1701 cm^{-1} ($[\text{N}_4\text{C}-\text{NH}_2]^-$, **10**), 1563 cm^{-1} ($[(\text{NO}_2)_3\text{Ph}-\text{O}]^-$, **11**) and at ≈ 1400 and 760 cm^{-1} ($[\text{N}_4\text{C}-\text{N}=\text{N}-\text{CN}_4]^{2-}$, **12a** and **12b**) [1b, 1h, 11c, 19, 25].

The vibrational (both IR and Raman) frequencies of the GU^+ cation were calculated and scaled as described above. Table S1 of the Supporting Information contains the calculated, scaled and measured frequencies of the cation in salts **6–12**. The measured frequencies were taken as a rough average of the observed signals in the IR and Raman spectra of all compounds. As expected, the calculated shifts at the highest wave numbers did not find a match in the experimental values. However, the rest of the calculated values found reasonably good agreement in the observed frequencies. NH stretching bands are very intense in the IR spectra and found in the range from ≈ 3200 to 3400 cm^{-1} . The stretching vibrations of the urea (C=O) and guanidine (C=N) moieties are coupled to deformation modes of the amino groups and found at ≈ 1740 and 1645 cm^{-1} , respectively. The range $1600\text{--}900 \text{ cm}^{-1}$ is mainly dominated by deformation modes of the three NH_2 groups and C–O and C–N stretching modes. The rocking vibrations of the guanidine and urea moieties are active both in the IR and Raman spectra of the compounds and found at $\approx 710 \text{ cm}^{-1}$. Below 700 cm^{-1} the spectra are again dominated by many in-plane and out-of-plane bending vibrations.

The ^1H NMR spectra of the compounds in $[\text{D}_6]\text{DMSO}$ show (in general) well resolved resonances for the hydrogen atoms in the GU^+ cation. They are observed at ≈ 10 (NH), 8 (NH_2^+) and 7 (NH_2) ppm as broad singlets. In the ^{13}C NMR spectra, the guanidine (CN_3) and the urea ($\text{C}(\text{O})\text{N}_2$) carbon atoms have similar shifts at ≈ 155 ppm and can not be differentiated. Because of the quadrupole broadening observed in the ^{14}N NMR

of the compounds, only highly symmetrical anions could be observed. Thus, the resonance of the nitrate anion was found at -5 ppm, whereas the azide anion showed the two common resonances for ionic azides at ≈ -140 and -270 ppm, the nitro-group of the 5-nitrotetrazolate anion resonates at -23 ppm and the nitro-groups of the picrate anion have a broad shift at -12 ppm. In order to observe the resonances of the cation, a ^{15}N NMR (natural abundance) was recorded (Figure 1). Apart from the shifts of the anion, the three nitrogen atoms attached to hydrogen atoms have highly negative resonances. The NH nitrogen atom resonates at the lowest field of all three at -272 ppm and appears as a doublet, whereas the two different NH_2 groups have very similar shifts at ≈ -300 ppm and are observed as two overlapping triplets. All three coupling constants (J) have similar values at ~ 90 Hz.

Crystal Structures

Single crystals of compounds **4**, **7** [19, **8a** and **10**, suitable for X-ray diffraction analysis, were grown as described in the experimental section. The X-ray crystallographic data sets were collected with an Oxford Diffraction Xcalibur 3 diffractometer equipped with a CCD detector using the CrysAlis CCD software [26]. All data were collected using graphite-monochromated $\text{Mo-K}\alpha$ radiation ($\lambda = 0.71073 \text{ \AA}$). The data reductions were performed with the CrysAlis RED software [27], and no absorption corrections were applied to data sets collected for any of the compounds. All structures were solved by direct methods using the suit of programs (SHELXS-97 and SIR92) available in the Wingx package [28–31], refined by means of full-matrix least-squares procedures using SHELXL-97 and finally checked using the program PLATON [32]. All non-hydrogen atoms were refined anisotropically. For all compounds all hydrogen atoms were located from difference Fourier electron-density maps and refined isotropically. The crystallographic data and refinement have been summarized in Table 1. Table 2 shows a summary of the bond lengths and angles for the GU^+ cation in the different compounds. The hydrogen-bonding geometries have been collected in the Supporting Information Table S2, whereas Tables S3 to S6 contain a full record of the graph-sets found in the structures. Further information concerning the crystal structure determinations in CIF format has been deposited at the Cambridge Crystallographic Data Centre [33].

The crystal structure of the perchlorate salt (**7**) has been previously reported in our group [19] and is only showed here for comparison purposes. Figure 2 shows the asymmetric unit of the compound, where the lone pair of the NH_2 nitrogen atom (N1) shows delocalization over to the carbonyl group, as reflected by a substantially shorter C1–N1 distance ($\sim 1.33 \text{ \AA}$) in comparison to the C1–N2 bond ($\sim 1.40 \text{ \AA}$). The C1–N1 bond character falls in-between that of a classical C1–N1 single bond (1.47 \AA) and that of a C1=N1 double bond (1.22 \AA) [34].

In contrast to the remainder of the compounds, the GU^+ cation in **4** is not planar. The urea and guanidine moieties are twisted in respect to each other [dihedral angle C2–N2–C1–O1 = $-15.1(2)^\circ$]. The formation of non-planar layers along the

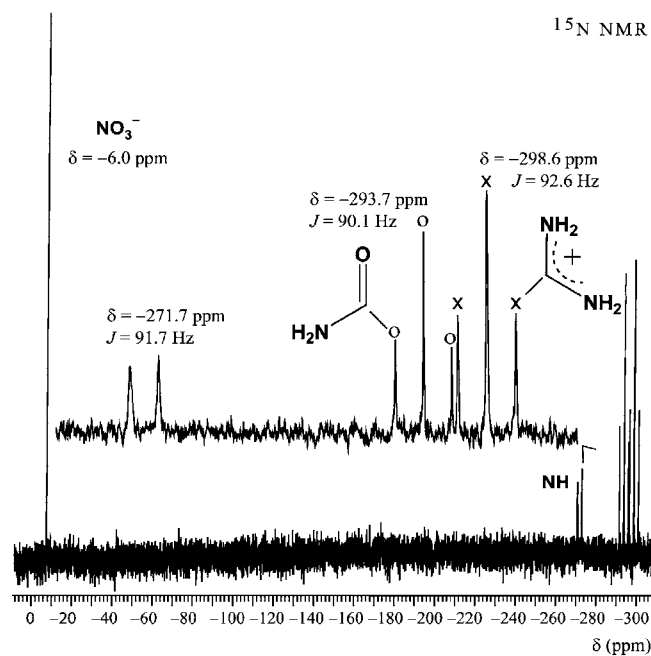


Figure 1. Coupled ^{15}N NMR of the guanilyurea cation in guanilyurea nitrate (**6**).

Table 1. Crystal structure solution and refinement for guanylurea salts **4**, **7**, **8a** and **10**.

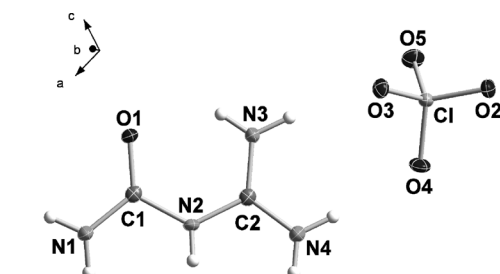
Parameter	4	7	8a	10
Empirical formula	C ₂ H ₇ N ₄ OCl	C ₂ H ₇ N ₄ O ₅ Cl	C ₂ H ₉ N ₇ O ₂	C ₃ H ₉ N ₉ O
Formula weight /g·mol ⁻¹	138.57	202.57	163.16	187.19
Temperature /K	100(2)	100(2)	100(2)	100(2)
Crystal size /mm	0.25 × 0.10 × 0.10	0.20 × 0.10 × 0.10	0.18 × 0.10 × 0.07	0.30 × 0.10 × 0.05
Crystal system	Monoclinic	Monoclinic	Monoclinic	Monoclinic
Space group	<i>P</i> 2 ₁ / <i>c</i>	<i>P</i> 2 ₁ / <i>c</i>	<i>P</i> 2 ₁ / <i>c</i>	<i>P</i> 2 ₁
<i>a</i> /Å	8.2515(3)	8.0115(2)	8.6403(3)	6.8425(5)
<i>b</i> /Å	10.7121(4)	9.7328(2)	6.6651(2)	4.8514(4)
<i>c</i> /Å	6.7703(3)	9.5770(2)	12.8932(6)	11.943(1)
α /°	90	90	90	90
β /°	108.53(1)	105.895(2)	102.29(1)	96.22(1)
γ /°	90	90	90	90
<i>V</i> _{UC} /Å ³	567.4(9)	718.21(3)	725.4(6)	394.1(3)
<i>Z</i>	4	4	4	2
ρ_{calc} /g·cm ⁻³	1.622	1.873	1.494	1.577
<i>m</i> /mm ⁻¹	0.575	0.527	0.127	0.126
<i>F</i> (000)	288	416	344	196
θ range /°	3.70–25.99	4.19–26.00	3.90–26.00	4.30–30.11
Index ranges	–10 ≤ <i>h</i> ≤ 10 –13 ≤ <i>k</i> ≤ 13 –8 ≤ <i>l</i> ≤ 8	–9 ≤ <i>h</i> ≤ 11 –12 ≤ <i>k</i> ≤ 11 –11 ≤ <i>l</i> ≤ 11	–10 ≤ <i>h</i> ≤ 10 –8 ≤ <i>k</i> ≤ 8 –15 ≤ <i>l</i> ≤ 15	–9 ≤ <i>h</i> ≤ 9 –6 ≤ <i>k</i> ≤ 6 –16 ≤ <i>l</i> ≤ 16
Reflections collected	5567	5373	7031	5346
Independent reflections	1115 (<i>R</i> _{int} = 0.0232)	1397 (<i>R</i> _{int} = 0.0214)	1421 (<i>R</i> _{int} = 0.0194)	1281 (<i>R</i> _{int} = 0.0335)
Data/Restraints/Parameters	1115/0/101	1397/0/137	1421/0/137	1281/0/154
Goodness-of-fit on <i>F</i> ²	1.089	1.098	1.106	0.831
<i>R</i> ₁ [<i>F</i> > 4 σ (<i>F</i>)]	0.0209	0.0257	0.0261	0.0287
<i>R</i> ₁ (all data)	0.0274	0.0286	0.0325	0.0516
<i>wR</i> ₂ [<i>F</i> > 4 σ (<i>F</i>)]	0.0494	0.0706	0.0721	0.0571
<i>wR</i> ₂ (all data)	0.0527	0.0718	0.0764	0.0585

$$R_1 = \frac{\sum ||F_o| - |F_c||}{\sum |F_o|}, R_w = \frac{[\sum (F_o^2 - F_c^2) / \sum w (F_o^2)]^{1/2}}{w}, w = [\sigma_c^2 (F_o^2) + (xP)^2 + yP]^{-1}, P = (F_o^2 - 2F_c^2) / 3.$$

Table 2. Selected bond lengths /Å and angles /° for guanylurea salts **4**, **7**, **8a** and **10**.

Distances	4	7	8a	10
N1–C1	1.331(2)	1.330(2)	1.332(1)	1.343(2)
C1–O1	1.234(2)	1.233(2)	1.227(1)	1.227(2)
C1–N2	1.398(2)	1.398(2)	1.400(1)	1.391(2)
N2–C2	1.357(2)	1.357(2)	1.360(1)	1.359(2)
C2–N3	1.312(2)	1.317(2)	1.313(1)	1.314(2)
C2–N4	1.323(2)	1.319(2)	1.319(1)	1.318(2)
Angles	4	7	8a	10
N1–C1–O1	124.8(1)	124.4(1)	124.1(1)	124.1(2)
N1–C1–N2	112.9(1)	113.6(1)	114.2(1)	112.3(2)
O1–C1–N2	122.2(1)	122.0(1)	121.5(1)	123.5(2)
C1–N2–C2	126.7(1)	126.0(1)	125.5(1)	125.9(2)
N2–C2–N3	122.2(1)	121.0(1)	121.2(1)	120.7(2)
N2–C2–N4	116.2(1)	117.8(1)	117.2(1)	117.6(2)
N3–C2–N4	121.4(1)	121.2(2)	121.4(1)	121.6(2)

b axis in the unit cell is represented in Figure 3. The “twisted” guanidine amino-group nitrogen atom (N4) joins the layers by forming hydrogen bonds to the chlorine atoms with N4–H4B...Clⁱⁱⁱ = 3.203(1) Å (symmetry code: (iii) 1 –*x*, –*y*, –*z*). Extensive hydrogen-bonding in a layer is found: every chlorine atom forms five hydrogen bonds to four different GU⁺ cations (Figure 4a). Together with the aforementioned hydrogen bond between layers, the coordination number through formation of hydrogen bridges around the chlorine atoms is six, describing

**Figure 2.** Asymmetric unit of **7** with the labeling scheme. Selected bond lengths /Å and angles /° for the ClO₄[–] anion: Cl–O₅ = 1.432(1), Cl–O₂ = 1.439(1), Cl–O₄ = 1.444(1), Cl–O₃ = 1.461(1) Å; O₅–Cl–O₂ = 110.3(1), O₅–Cl–O₄ = 110.2(1), O₂–Cl–O₄ = 110.2(1), O₅–Cl–O₃ = 109.4(1), O₂–Cl–O₃ = 108.9(1), O₄–Cl–O₃ = 107.9(1)°.

a distorted pentagonal basal pyramid, with distances between donor and acceptor atoms in the range ≈ 3.15–3.30 Å, well within the sum of the van der Waals radii (*r*_N + *r*_{Cl} = 3.30 Å) [35]. Graph-set analysis [36] facilitates the description of the complex hydrogen-bonding networks found in the structure of **4**. At the primary level, six **D1,1(2)**, two **C1,1(2)** and the usual **S(6)** patterns are identified by *RPLUTO*. At the secondary level, dimer **D3,2(9)** and **D3,3(X)** (*X* = 11, 13), chain **C1,2(X)** (*X* = 4, 6, 8) and **C2,2(12)** and ring **R1,2(6)** and **R2,4(X)** (*X* = 12, 16) graph-sets are found. Some of these patterns resemble those of the azide salt **8a** (see below), for example, the **R1,2(6)** pattern (Figure 4b) is formed by the urea half of the

cation (the guanidine half in the azide salt) with $N2\cdots Cl = 3.159(1)$ Å and $N1\cdots Cl = 3.318(1)$ Å. Other graph-sets are characteristic of the chloride salt, such as the **R2,4(12)** network formed by the hydrogen bond between layers.

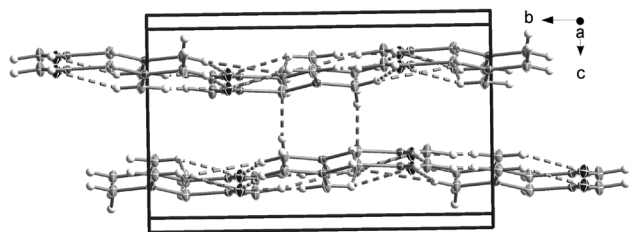


Figure 3. View of the unit cell of compound **4** along the *a* axis showing the hydrogen-bonding in a layer and between layers (dotted lines).

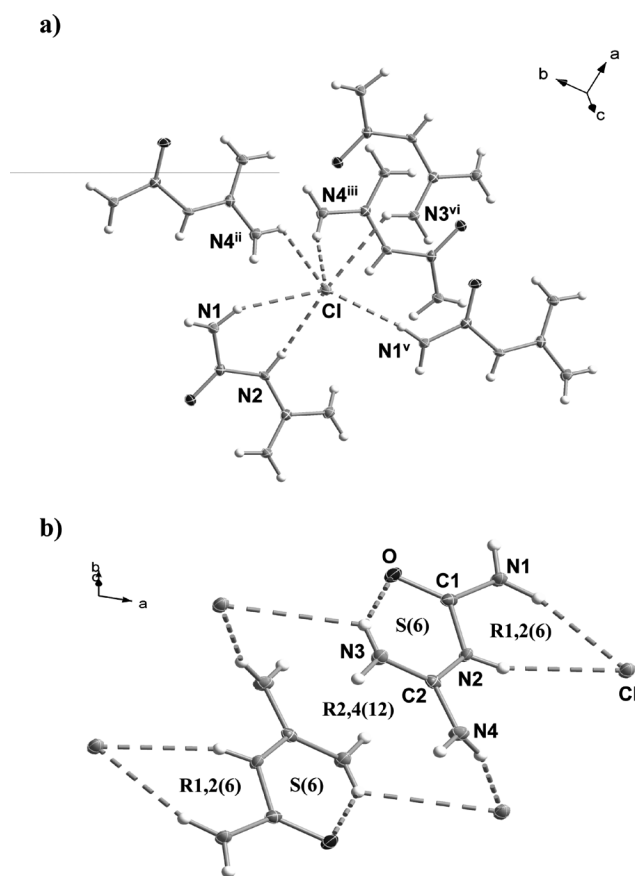


Figure 4. Hydrogen-bonding around the chloride anion in the crystal structure of compound **4** and b) representative hydrogen-bonding networks. Symmetry codes: (ii) $1 -x, 0.5+y, 0.5-z$; (iii) $1 -x, -y, -z$; (v) $1 -x, -0.5+y, 0.5-z$; (vi) $1+x, y, z$.

Guanylurea azide crystallizes as the monohydrate compound (**8a**) forming the twelve medium-to-strong hydrogen bonds summarized in Table S5, ten of which are normal dimeric interactions of the type **D1,1(2)** (primary level). On the other hand, one of the amino group nitrogen atoms in the cation forms one **C1,1(6)** chain graph-set with one of the azide nitrogen atoms with a long hydrogen bond ($N4\cdots N5^{iii} = 3.342(1)$ Å;

symmetry code: (iii) $1 -x, 1 -y, -z$) and the intramolecular hydrogen bond ($N3\cdots O1 = 2.647(1)$ Å) is described by an **S(6)** motif. At the secondary level, most of the hydrogen-bonding networks are described by finite patterns of the type **D1,2(3)**, **D2,2(X)** ($X = 4, 5, 7, 9$), **D3,2(9)** and **D3,3(X)** ($X = 11, 13$). However, there exist many **C1,2(X)** ($X = 6, 8$) and **C2,2(X)** ($X = 6, 7, 9$) chain patterns and **R2,1(3)**, **R1,2(6)** and **R4,4(X)** ($X = 12, 16, 18$) graph-sets. Some of these networks are represented in Figure 5. The **R1,2(6)** motifs are formed between $N4H_2$, which describes the chain pattern discussed above and $N2H$ of the cation by interaction to one of the azide anion nitrogen atoms ($N2\cdots N5^{iii} = 2.897(1)$ Å).

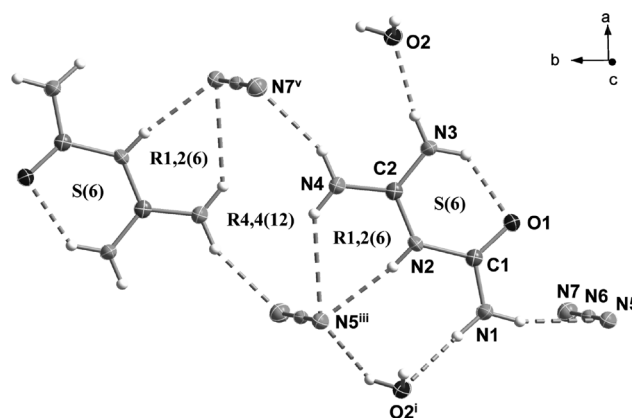


Figure 5. Hydrogen-bonding around the GU^+ cation in the crystal structure of compound **8a** showing the formation of some characteristic graph-sets. Selected bond lengths /Å and angles /° for the N_3^- anion: $N6-N5 = 1.182(1)$, $N6-N7 = 1.176(1)$ Å; $N5-N6-N7 = 178.7(1)^\circ$.

Two cations placed on contiguous layers interact over “azide-bridges” to form an **R4,4(12)** graph-set, again via the hydrogen bond between $N4$ and $N5^{iii}$ and also between $N4$ and $N7^v$ ($N4\cdots N7^v = 3.013(1)$ Å; symmetry code: (v) $1+x, 1+y, z$). In the unit cell (Figure 6) there are layers of cations, which are approximately parallel to the *a* direction whereas the azide anions are parallel to the *c* axis and, thus, perpendicular to the cations. The crystal water molecules act as hydrogen-bond donors joining the anions ($O2\cdots N7^{vii} = 2.826(1)$ Å and $O2\cdots N5^{viii} = 2.826(1)$ Å; symmetry codes: (vii) $2 -x, 0.5+y, 0.5-z$; (viii) $2 -x, 1 -y, -z$) and as hydrogen-bond acceptors joining the cations ($N3\cdots O2 = 2.824(1)$ Å and $N1\cdots O2^i = 2.951(1)$ Å; symmetry code: (i) $-1+x, y, z$) and forming a complex three dimensional hydrogen-bonded network.

Figure 7 shows the asymmetric unit with the labeling scheme for salt **10**. In contrast to 5-aminotetrazolium salts (i.e., positively charged tetrazole ring) in which the amino group is approximately coplanar with the tetrazole ring, the amino group in the 5-aminotetrazolate anion has a marked sp^3 character [e.g., $C-NH_2$ distance in 5-aminotetrazolium nitrate is with $1.308(2)$ Å, much shorter than that found in **10** for which $C3-N7 = 1.380(2)$ Å] [37a], keeping in with alkali metal salts containing the same anion [37b]. The non-planarity of the anion accounts for the non-formation of layers in the structure as shown in Figure 7b. The amino groups in the guanylurea cat-

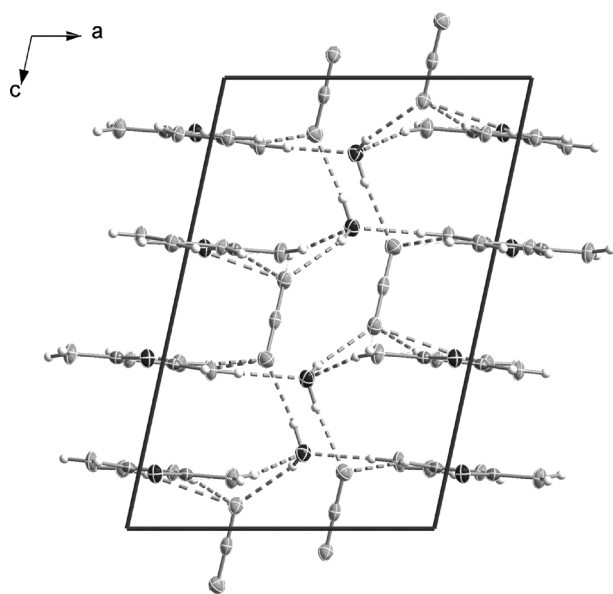


Figure 6. View of the unit cell of compound **8a** along the *b* axis showing the hydrogen-bonding in the structure (dotted lines).

ion are sp^2 hybridized and thus the structure of the cation is planar [dihedral angle $N1-C1-N2-C2 = 175.7(2)^\circ$].

There exists however extensive hydrogen-bonding in the structure (Table S2). The hydrogen-bonding around one of the GU^+ cations is represented in Figure 8. Every cation is surrounded by other cations and anions so that every hydrogen atom is involved in the formation of hydrogen bridges. Using graph-set analysis, the primary hydrogen-bonding network is described by dimeric **D1,1(2)** and chain **C1,1(4)** motifs, as well as the usual **S(6)** graph-set ($N4 \cdots O = 2.703(2) \text{ \AA}$). The secondary level network is formed by several **D3,3(X)** ($X = 7, 9, 10, 11, 15$) finite chain, **C2,2(X)** ($X = 6-11$) infinite chain and (more interestingly) by **R2,1(3)**, **R1,2(6)** and **R2,2(X)** ($X = 6, 7$) ring patterns. Some of the ring graph-sets are also represented in Figure 8. For example, N1 forms two weak hydrogen bonds to the same anion ($N1 \cdots N7^{vi} = 3.293(3) \text{ \AA}$ and $N1 \cdots N8^{vi} = 3.236(3) \text{ \AA}$; symmetry code: (vi) $x, 1+y, z$) describing an **R2,1(3)** graph-set, whereas the interaction between N1 and N2 with $N8^{vi}$ yields a **R1,2(6)** pattern and the combination of both results in the formation of a larger **R2,2(7)** network.

Thermal and Energetic Properties

Electronic energies for all anions and the guanylurea cation were calculated using Møller-Plesset perturbation theory truncated at the second order (MP2)[21] and were used unscaled. The results of the MP2 electronic energy calculations are tabulated in the Supporting Information (Table S7). As for the vibrational frequencies calculations (see above) the correlation consistent polarized double-zeta basis set cc-pVDZ was also used [23, 24].

The physical and chemical properties of all compounds in this study (**6-12**) have been collected in Table 3. As proved by DSC measurements, all compounds have high thermal sta-

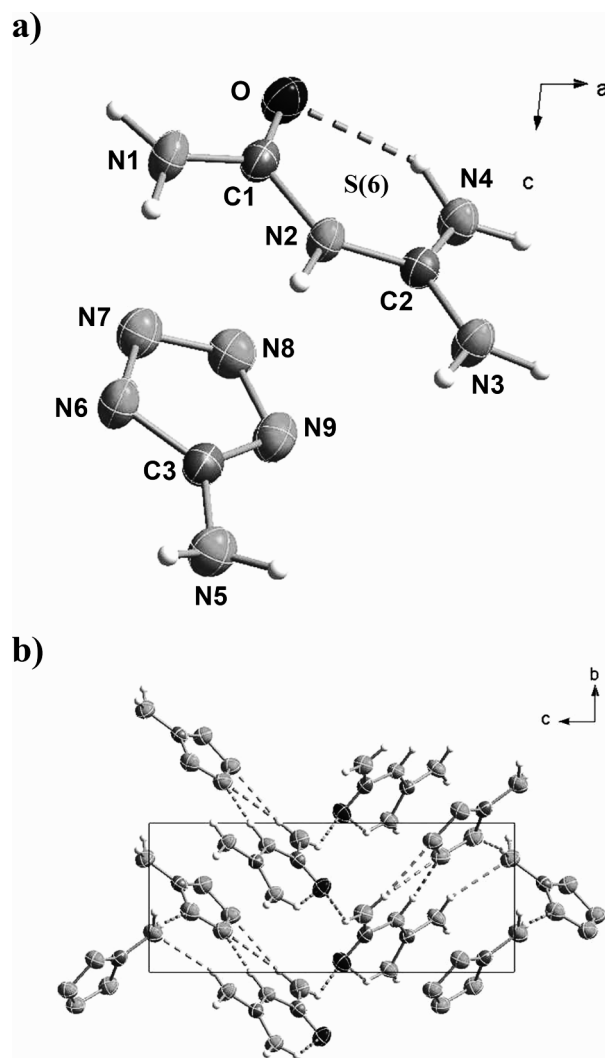


Figure 7. Asymmetric unit of **10** with the labeling scheme and b) view along the *a* axis showing the formation of hydrogen bonds (dotted lines) in the unit cell. Selected bond lengths / \AA and angles / $^\circ$ for the $[N_4C-NH_2]^-$ anion: $C3-N5 = 1.380(2)$, $C3-N6 = 1.326(2)$, $N6-N7 = 1.356(2)$, $N7-N8 = 1.300(2)$, $N8-N9 = 1.351(2)$, $N9-C3 = 1.328(2) \text{ \AA}$; $N5-C3-N6 = 124.0(2)$, $C3-N6-N7 = 104.7(1)$, $N6-N7-N8 = 108.7(1)$, $N7-N8-N9 = 110.2(1)$, $N8-N9-C3 = 104.0(1)$, $N9-C3-N5 = 123.5(2)$, $N9-C3-N6 = 112.2(2)^\circ$.

bilities as suggested by their high decomposition points ranging from 180°C (**8a** and **8b**) to 253°C (**11**). All salts show sharp decomposition without melting (two sharp decomposition steps in the case of the 5,5'-azoatetrazolate salts **12a** and **12b**), with the only exception of the 5-aminotetrazolate salt (**10**), which has a high melting point at 152°C and an even higher decomposition temperature at 240°C , making for a relatively large liquid range ($\sim 90^\circ\text{C}$). The loss of the water of crystallization in the hydrated salts **8a** and **12a** is indicated by an endothermic peak at $\sim 100^\circ\text{C}$ in the case of **8a**, whereas this is not observable from the DSC curve of compound **12a**. Unfortunately, the high insolubility of **12a** in all tested solvents did not allow the obtaining of measurable single crystals of the compound. We assume that the solvent water remains in the

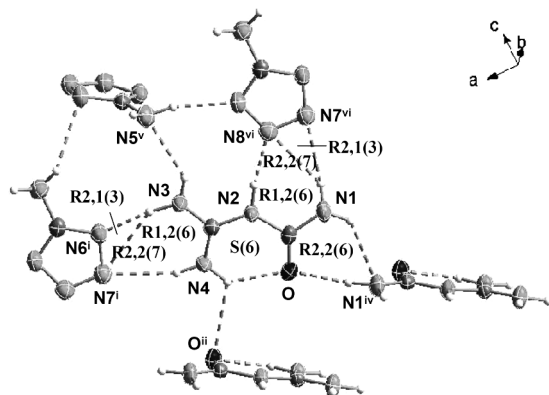


Figure 8. Hydrogen-bonding around the GU^+ cation in the crystal structure of **10** showing the formation of some characteristic graph-sets.

a picnometer (**6**, **8b**, **9**, **11**, **12a** and **12b**) or calculated using X-ray diffraction techniques (**7**, **8a** and **10**). The density values range between moderate ($\rho(\mathbf{8a}) = 1.494 \text{ g}\cdot\text{cm}^{-3}$) and high ($\rho(\mathbf{7}) = 1.873 \text{ g}\cdot\text{cm}^{-3}$) and are in the range between those of recently reported energetic salts with the 5,5'-azotetrazolate anion ($\rho \sim 1.5 \text{ g}\cdot\text{cm}^{-3}$) [1b, 11b] and that of the high explosive octogen (HMX, $\rho = 1.905 \text{ g}\cdot\text{cm}^{-3}$) [39].

For each salt (**6–12**), the constant volume energy of combustion was predicted on the basis of calculated electronic energies (see “Computational Methods” section above) and an estimation of lattice enthalpy [40] using similar methods to those reported in the literature [41]. The predicted thermochemical properties are also summarized in Table 3. Apart from salts **6** and **11**, which have negative energies of formation, the remainder of the compounds, either formed by the highly oxidant perchlorate anion (**7**) or by highly endothermic moieties, i.e., azide (**8a** and **8b**) or tetrazolate (**9**, **10**, **12a** and **12b**) anions, have positive heats of formation. In particular, the 5,5'-azotet-

Table 3. Physical and chemical properties of guanylurea salts **6–12**.

	6	7	8a	8b	9	10	11	12a	12b
Formula	$\text{C}_2\text{H}_7\text{N}_5\text{O}_4$	$\text{C}_2\text{H}_7\text{N}_4\text{O}_5\text{Cl}$	$\text{C}_2\text{H}_9\text{N}_7\text{O}_2$	$\text{C}_2\text{H}_7\text{N}_7\text{O}$	$\text{C}_3\text{H}_7\text{N}_9\text{O}_3$	$\text{C}_3\text{H}_9\text{N}_9\text{O}$	$\text{C}_8\text{H}_9\text{N}_7\text{O}_8$	$\text{C}_6\text{H}_{15}\text{N}_{18}\text{O}_{2.5}$	$\text{C}_6\text{H}_{14}\text{N}_{18}\text{O}_2$
Mol. Mass / g mol^{-1}	165.05	202.01	163.08	145.07	217.07	187.09	331.05	379.16	370.15
$T_m / ^\circ\text{C}^{\text{a}}$						152			
$T_d / ^\circ\text{C}^{\text{b}}$	203	204	180	180	209	240	253	213	199
$N / \%$ ^c	42.4	27.7	60.1	67.6	58.1	67.4	29.6	66.5	68.1
$N + O / \%$ ^d	81.2	67.3	79.7	78.6	80.1	75.9	68.3	77.0	76.7
$\Omega / \%$ ^e	-33.9	-15.8	-63.8	-71.7	-47.9	-81.2	-60.4	-71.7	-73.5
$\rho / \text{g}\cdot\text{cm}^{-3}$ ^f	1.567*	1.873	1.494	1.499*	1.615*	1.577	1.669*	1.599*	1.588*
$-\Delta U_{\text{comb}} / \text{cal}\cdot\text{g}^{-1}$ ^g	1987	1851	3078	2995	2442	3273	2928	3354	3343
$\Delta U_{\text{f}}^\circ / \text{kJ}\cdot\text{kg}^{-1}$ ^h	-2392	+88	+303	+341	+282	+623	-1046	+2267	+2322
$\Delta H_{\text{f}}^\circ / \text{kJ}\cdot\text{kg}^{-1}$ ⁱ	-2512	-4	+190	+213	+174	+497	-1136	+2157	+2208

a, b) Melting (T_m) and decomposition (T_d) points from DSC measurements carried out at a heating rate of $\beta = 5 \text{ }^\circ\text{C}\cdot\text{min}^{-1}$. c) Nitrogen contents. d) Combined nitrogen and oxygen contents. e) Oxygen balance. f) Calculated density from X-ray measurements or experimentally determined from picnometer experiments (*). g) Constant volume energy of combustion. h) Energy of formation. i) Heat of formation. g, h, i) Values predicted based on electronic energies and using the MP2 method.

structure until decomposition, which would account for the difference in the decomposition temperatures between the two 5,5'-azotetrazolate salts **12a** (213 $^\circ\text{C}$) and **12b** (199 $^\circ\text{C}$). Lastly, the trend in the decomposition points of **6–12** (**11** > **10** > **12a** > **9** > **6** ~ **7** > **12b** > **8a** = **8b**) is in agreement with other studies with salts containing similar anions [1b, 11b, 25d, 25e, 38].

The nitrogen contents and particularly the combined nitrogen plus oxygen percentages of salts **6–12** are relatively high and vary between 67.3 % (**7**) and 81.2 % (**6**), suggesting the possibility to form large amounts of environmentally benign or less malign gaseous products (i.e., N_2 and CO_2). On the other hand, the oxygen contents (Ω) vary over a large range. The perchlorate salt (**7**), for which $\Omega = -15.8 \%$, has a value slightly less negative than that of commonly used cyclotrimethylenetrinitramine (RDX, $\Omega = -22 \%$), whereas that of the 5-aminotetrazolate salt (**10**, $\Omega = -81.2 \%$) is slightly more negative than that of 1,3,5-trinitrotoluene (TNT, $\Omega = -74 \%$). Since density of new energetic materials is a crucial parameter in determining their performance (see discussion below), the densities of all compounds were either measured experimentally by using

razolate salts **12a** and **12b** possess highly positive calculated values ($\Delta U_{\text{f}}^\circ \sim 2300 \text{ kJ}\cdot\text{kg}^{-1}$), comparable to the high explosive 1-azido-2-nitro-2-azapropene (ANAP, $\Delta U_{\text{f}}^\circ = 2381 \text{ kJ}\cdot\text{kg}^{-1}$). From the energies of formation (back-calculated from MP2 method predicted combustion data), the densities (from picnometer or X-ray diffraction measurements) and the molecular formulas of compounds **6–12**, the performance of all materials, typically measured by their detonation parameters, i.e., detonation pressure (P) and detonation velocity (D) and their specific impulse (I_{sp}), was predicted using the EXPLO5 computer program (see Supporting Information) [42]. The results of the calculations have been collected in Table 4 together with some initial safety testing results of importance and the corresponding values for FOX-12 (guanylurea dinitramide) for comparison purposes. Once again, the change in the anion is reflected in the performance values. Nitrate salt **6**, which has the most negative heat of formation of all materials in this study, shows accordingly low detonation parameters ($P = 17.4 \text{ GPa}$, $D = 7004 \text{ m}\cdot\text{s}^{-1}$), which are nevertheless similar to those of commonly used TNT ($P = 19.4 \text{ GPa}$, $D = 7073 \text{ m}\cdot\text{s}^{-1}$ at a density of $1.60 \text{ g}\cdot\text{cm}^{-3}$). The trend in the

Table 4. Predicted detonation and combustion parameters (using the EXPLO5 code) and sensitivity data for guanylurea salts **6–12**.

	$T_{\text{ex}} / \text{K}^{\text{a}}$	$V_0 / \text{L} \cdot \text{kg}^{-1} \text{ b)}$	$P / \text{GPa}^{\text{c}}$	$D / \text{m} \cdot \text{s}^{-1} \text{ d)}$	Impact / J^{e}	Friction / N^{e}	ESD (+/-) ^{f)}	Thermal Shock ^{g)}	I_{sp} / s ^{h)}
6	2624	858	17.4	7004	>40	>360	–	Burns	177
7					>40	>360	–	Deflagrates	
8a	2642	917	20.6	7880	>40	>360	–	Deflagrates	170
8b	2129	875	16.9	7289	>40	>360	–	Deflagrates	165
9	2944	801	20.3	7439	>40	>360	–	Burns	183
10	2085	854	18.4	7530	>40	>360	–	Burns	165
11	3158	688	19.7	7152	>40	>360	–	Burns	161
12a	3034	816	24.3	8222	>40	>360	–	Burns	210
12b	2957	805	23.3	8115	>40	>360	–	Burns	206
FOX-12 ⁱ⁾	3372	848	27.6	8308	32	>350	–	Deflagrates	210

a) Temperature of the explosion gases; b) Volume of the explosion gases; c) Detonation pressure; d) Detonation velocity; e) Impact and friction sensitivities according to standard BAM methods [45], f) Sensitivity to electrostatic discharge (~20 kV), + sensitive, – insensitive (using a Tesla coil V-24); g) Response to fast heating in the “flame test”; h) Specific impulse; i) The values for FOX-12 (guanylurea dinitramide) have been calculated using the EXPLO5 code [42] from its energy of formation, calculated from its heat of formation ($\Delta H_{\text{f}}^{\circ} = -355 \text{ kJ} \cdot \text{mol}^{-1}$) [13].

increase of the detonation parameters is in agreement with the density and heats of formation, which are the two parameters of which performance is most dependant upon [39, 43] Compounds **12a** ($P = 24.3 \text{ GPa}$, $D = 8222 \text{ m} \cdot \text{s}^{-1}$) and **12b** ($P = 23.3 \text{ GPa}$, $D = 8115 \text{ m} \cdot \text{s}^{-1}$), which have the highest (positive) heats of formation, have also the largest detonation parameters, similar to FOX-12 ($P = 27.6 \text{ GPa}$, $D = 8308 \text{ m} \cdot \text{s}^{-1}$), which has been developed as a “high performance insensitive ammunition” [13, 14]. All compounds are also higher performing than recently developed polycyano compounds regardless of the higher positive heats of formation of the latter [44]. Although relatively low, the specific impulses computed for compounds **6–12** are higher than those expected for polycyano-based molecules [44] and the 5,5'-azotetrazolate salts **12a** and **12b** exhibit values perfectly comparable to that of FOX-12 ($I_{\text{sp}} = 210 \text{ s}$). Sensitivity testing using standard BAM tests [45] revealed marked insensitivity for all compounds, which are neither impact (>40 J) nor friction sensitive (>360 N), which is a clear advantage in terms of safety in comparison with new tetrazolium-based energetic materials with comparable anions [1h, 11c] or commonly used RDX (impact = 7 J, friction = 120 N) [39]. In addition, all **6–12** are insensitive to an electrostatic discharge of ~20 kV. Lastly, the perchlorate (**7**) and the azide (**8a** and **8b**) salts deflagrate when put into sudden contact with the flame of a Bunsen burner (“flame test”), similar to the dinitramide salt (FOX-12), whereas the remainder of the salts burn nicely giving little or no smoke.

The detonation parameters for formulations of the guanylurea salts **6–12** with an oxidant such as ammonium nitrate (AN) or ammonium dinitramide (ADN) were also calculated using the EXPLO 5 code and are tabulated in the Supporting Information (Tables S8 and S9). The formulations calculated were composed of compound and oxidant in oxygen neutral ratios. Mixtures of **6–12** with AN (Table S8) generally show an increase in the detonation parameters in respect to the stand-alone compounds and in compounds to values not significantly different from those predicted for TNT formulations with AN ($P = 25.4 \text{ GPa}$, $D = 8086 \text{ m} \cdot \text{s}^{-1}$), whereas mixtures with ADN

(Table S9) have a much better predicted performance, again reaching valuable comparable to mixtures of TNT and ADN ($P = 31.7 \text{ GPa}$, $D = 8739 \text{ m} \cdot \text{s}^{-1}$). In all cases, the performances predicted for formulations of **6–12** with AN or ADN, are higher than those of AN ($P = 15.1 \text{ GPa}$, $D = 6602 \text{ m} \cdot \text{s}^{-1}$) or ADN ($P = 22.7 \text{ GPa}$, $D = 7650 \text{ m} \cdot \text{s}^{-1}$) alone.

Long-term Stability and Decomposition Gases

Because of the interesting energetic properties of the 5,5'-azotetrazolate salt **12a**, i.e., high decomposition temperature, high nitrogen content, low sensitivity and relatively high performance, the long-term stability of the compound was assessed using a Systag FlexyTSC instrument (thermal safety calorimetry) [46] in combination with a RADEX V5 oven and the SysGraph software. An amount of ~0.5 g of finely divided and homogeneous sample of the material was loaded in a glass test-vessel at atmospheric pressure. The substance was then tempered at ~50 °C below its decomposition point (from the DSC measurements) for 48 hours. Figure 9 shows the thermal safety calorimetry (TSC) curve of **12a**. At a temperature of ~160 °C, the TSC curve of the salt looks identical to that of the oven and visual inspection of the sample shows no apparent change in color or decomposition. This result can be extrapolated to a shelf live of above 15 years at room temperature, which is attractive when thinking about a possible application.

Using the densities of compounds **6–12** (either calculated from X-ray or observed from picnometer measurements), their molecular formulas and the calculated heats of formation, the ICT code [47] was used to predict the heats of explosion and the decomposition gases of the guanylurea salts in this work. The predicted values have been collected in Table 5.

The ICT code predicts the formation of large amounts of environmentally friendly molecular nitrogen (~270–580 $\text{g} \cdot \text{kg}^{-1}$), which is the main decomposition product for all compounds and, in particular, for the nitrogen-richest 5,5'-azotetrazolate salts (**12a** and **12b**). After this, H_2O , NH_3 and C (soot) are, in general, expected to be formed in largest

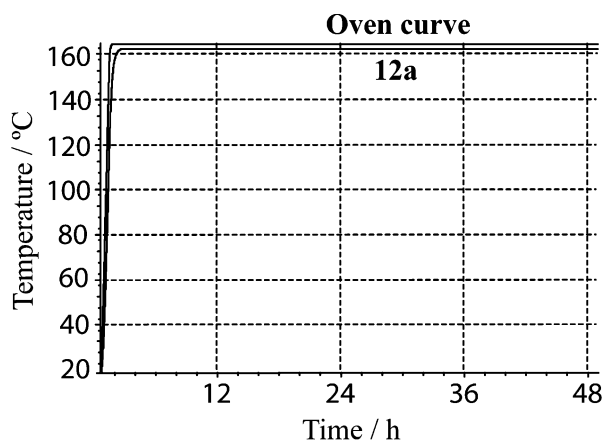


Figure 9. Thermal safety calorimetry plot of 5,5'-azotetrazolate salt **12a**.

Table 5. ICT-code predicted heats of explosion (ΔH_{ex} , $\text{cal}\cdot\text{g}^{-1}$) and decomposition gases ($\text{g}\cdot\text{kg}^{-1}$) for guanylurea salts **6–12**.

Compound	CO ₂	H ₂ O	N ₂	CO	H ₂	NH ₃	CH ₄	HCN	C	ΔH_{ex}
6	102.7	341.6	407.4	16.2	0.6	20.0	1.1	0.5	109.3	927
7	217.1	255.7	271.8	17.0	0.2	5.6	180.0	^{a)} 0.3	51.7	1549
8a	3.2	216.2	481.8	3.0	2.4	144.2	13.5	1.1	134.4	966
8b	1.1	122.0	547.2	1.8	2.6	155.4	18.9	1.1	149.8	625
9	27.7	220.7	551.0	8.3	0.9	35.4	2.4	0.7	152.6	958
10	0.6	94.9	534.7	1.3	2.7	168.1	21.0	1.1	175.5	604
11	228.6	227.4	290.6	31.5	0.5	6.4	1.0	0.3	213.2	1104
12a	1.5	116.2	564.1	2.0	2.0	121.6	12.8	1.0	178.7	1042
12b	1.1	95.2	580.0	1.7	2.1	122.0	14.5	1.0	182.3	977

a) No CH₄ and instead HCl was predicted for the perchlorate salt (**7**).

amounts. In particular, in the case of the better oxygen balanced salts **6**, **7** and **11** the amount of carbon atoms, which can be potentially oxidized to CO₂ (>100 $\text{g}\cdot\text{kg}^{-1}$) is markedly larger than for the remainder of the salts. In addition, highly toxic gases such as HCN or CO are only foreseen to form in small amounts. On the other hand, the only slightly negative oxygen balance of perchlorate salt **7** ($\Omega = -15.8\%$), accounts for the small amounts of C (soot) calculated, however, relatively large amounts of HCl gas are computed. In any case, compound **7** exhibits the highest calculated density of all compounds in this work ($\rho = 1.873\text{ g}\cdot\text{cm}^{-3}$), which correlates well with its highest heat of explosion ($\Delta H_{\text{ex}} = 1549\text{ cal}\cdot\text{g}^{-1}$), perfectly comparable to that of 1,3,5-trinitroperhydro-1,3,5-triazine (RDX, $\Delta H_{\text{ex}} = 1593\text{ cal}\cdot\text{g}^{-1}$), whereas, with the exception of salts **8b** and **10**, high heats of explosions above 900 $\text{cal}\cdot\text{g}^{-1}$ are expected for the rest of the materials discussed in this work.

Conclusions

Convenient syntheses for salts based on the guanylurea cation ($[\text{C}_2\text{H}_7\text{N}_4\text{O}]^+$) are reported. The new compounds were characterized by analytical and spectroscopic methods and the crystal structure of the $[\text{C}_2\text{H}_7\text{N}_4\text{O}]^+$ cation was determined for

compounds **4**, **7**, **8a** and **10**. The hydrogen-bonding networks in the solid-state structure are described fully in the formalism of graph-set analysis, showing interesting patterns. Standard BAM tests revealed a new family of compounds with low sensitivity towards impact, friction, electrostatic discharge and fast heating, and the robustness of the cation accounts for the high decomposition points of **6–12** ($T_d \geq 180\text{ }^\circ\text{C}$). The heats of formation of all salts were predicted by way of quantum chemical calculation (MP2) of electronic energies and their detonation parameters were calculated using the EXPLO5 code giving values comparable to commonly used energetic materials. Additionally, most of the compounds are predicted to decompose giving large amounts of environmentally friendly molecular nitrogen (ICT code). Lastly, the 5,5'-azotetrazolate salt **12a** also shows great long-term thermal stability (TSC) in addition to good thermal stability (DSC), high nitrogen content, low sensitivity and a relatively high performance, suggesting its potential for application

Experimental Section

Caution! Tetrazoles and nitrogen-rich materials are highly endothermic compounds and tend to explode under certain conditions. The synthesis and handling of the salts reported here should only be carried out by expert personnel. In particular, silver azide is a highly explosive solid and should never be dried nor used in large quantities. The use of safety equipment such as Kevlar gloves, leather coat, face shield and ear plugs is recommended and large scale synthesis is discouraged for all compounds.

General: See Supporting Information.

Guanylurea Chloride (4): Cyanoguanidine (6.089 g, 72.0 mmol) was dissolved in water (50 mL) in a 250 mL round-bottomed flask and concentrated hydrochloric acid (30 mL, 364.0 mmol, 37 %) was added slowly by means of a dropping funnel. Afterwards, the reaction mixture was heated to boiling and left to react for 15 min at this temperature and the solvent and excess HCl were removed by storing the solution in an oven at 80 °C for 2 days. The colorless solid left behind was pure by elemental analysis and the yield is approximately quantitative (9.838 g). Single crystals suitable for X-ray analysis were obtained when a diluted solution of the chloride salt **4** in water was left to evaporate slowly. $\text{C}_2\text{H}_7\text{N}_4\text{OCl}$ (138.03 $\text{g}\cdot\text{mol}^{-1}$) calcd.: C 17.39, H 5.11, N 40.58; found: C 17.07, H 5.01, N 40.42; DSC (5 °C·min⁻¹) (°C): 168 (m. p. + dec). **IR** (KBr): $\tilde{\nu} = 3410$ (vw) 3378(vw) 3251(vw) 3143(m) 2989(vw) 1693(vs) 1622(s) 1571(m) 1535(m) 1462(w) 1339(m) 1129(w) 1075(w) 931(vw) 742(m) 718(w) 692(m) 649(s) 606(s) 584(s) 579(s) 561(s) cm^{-1} . **Raman** (400 mW, 25 °C) $\tilde{\nu} = 3191$ (9) 1726(21) 1624(14) 1588(7) 1466(11) 1345(4) 1136(18) 1086(24) 1007(9) 940(29) 758(8) 694(18) 565(16) 504(6) 456(25) 437(37) 270(11) 175(15) 140(14) cm^{-1} . **¹H NMR** ($[\text{D}_6]$ DMSO, 25 °C): $\delta = 10.4$ (s, 1 H, NH), 8.2 (s, 4 H, NH₂), 7.2 (s, 2 H, NH₂). **¹³C NMR** ($[\text{D}_6]$ DMSO, 25 °C): $\delta = 155.6$ (1C, C1/C2), 154.5 (1C, C2/C1). **MS** m/z (FAB⁺, xenon, 6 keV, glycerine matrix): 103.1 (59, $[\text{C}_2\text{H}_7\text{N}_4\text{O}]^+$), 205.1 (4, $\{[\text{C}_2\text{H}_7\text{N}_4\text{O}]^+_2 - \text{H}^+\}$), 241.1 (13, $\{[\text{C}_2\text{H}_7\text{N}_4\text{OCl}] \cdot [\text{C}_2\text{H}_7\text{N}_4\text{O}]^+\}$).

Guanylurea Nitrate (6): Compound **6** was synthesized as described in ref. [19] in a 97 % yield. The elemental analysis and NMR spectroscopic data are in agreement with the previously reported data. $\text{C}_2\text{H}_7\text{N}_5\text{O}_4$ (165.05 $\text{g}\cdot\text{mol}^{-1}$) calcd.: C 14.54, H 4.27, N 42.42 %; found: C 14.48, H 4.17, N 42.21 %. **¹H NMR** ($[\text{D}_6]$ DMSO, 25 °C):

$\delta = 9.51$ (s, 1 H, NH), 8.13 (s, 4 H, NH₂), 7.14 (s, 2 H, NH₂). ¹³C NMR ([D₆]DMSO, 25 °C): $\delta = 155.6$ (1C, C1/C2), 154.5 (1C, C2/C1).

Guanylurea Perchlorate (7): Compound **7** was synthesized as reported previously [19] in a 91 % yield. Both elemental analysis and NMR spectroscopic data agree with the published data. C₂H₇N₄O₅Cl (202.01 g·mol⁻¹) calcd.: C 11.88, H 3.49, N 27.73 %; found: C 11.72, H 3.45, N 27.591 %. ¹H NMR ([D₆]DMSO, 25 °C): $\delta = 9.61$ (s, 1 H, NH), 8.02 (s, 4 H, NH₂), 7.04 (s, 2 H, NH₂). ¹³C NMR ([D₆]DMSO, 25 °C): $\delta = 155.5$ (1C, C1/C2), 154.4 (1C, C2/C1).

Guanylurea Azide Monohydrate (8a): The reaction was conducted in parallel attempts for four times in the following manner: in a plastic beaker (!) sodium azide (0.325 g, 5.0 mmol) was dissolved in water (6 mL) and a solution of silver nitrate (0.850 g, 5.0 mmol) in water (6 mL) was added. **Highly sensitive silver azide** precipitated immediately. The suspension was stirred for 15 min, filtered through gravity and the insoluble solid was washed with water to rinse any traces of unreacted sodium azide or silver nitrate. Meanwhile, compound **4** (0.650 g, 4.71 mmol) was dissolved in water (10 mL) in a plastic beaker (!) and the silver azide was carefully rinsed into the reaction flask with water. The reaction mixture was stirred for 2 h., heated shortly to boiling and the insoluble silver chloride and excess silver azide were filtered hot yielding a slightly yellow solution. The four filtrates were combined and rotavaporated until a colorless solid started to precipitate. At this point, the insoluble solid was dissolved by shortly heating to boiling and the solution left to slowly cool down yielding crystals of the azide salt as the monohydrate species (2.292 g, 75 %). X-ray quality crystals of the monohydrated species **8a**, were obtained by slow evaporation of an aqueous solution of the compound. C₂H₉N₇O₂ (163.14 g·mol⁻¹) calcd.: C 14.72, H 5.56, N 60.11 %; found: C 14.58, H 5.51, N 59.72 %; DSC (5 °C·min⁻¹ °C): ~100 (-H₂O), ~180 (m. p. + dec). IR (KBr): $\tilde{\nu} = 3342$ (vs) 3168(vs) 2343(vw) 2114(m) 2042(vs) 1727(vs) 1698(s) 1671(s) 1645(vs) 1594(vs) 1532(s) 1454(s) 1400(s) 1384(s) 1350(s) 1180(m) 1131(m) 1107(m) 1087(m) 1050(m) 928(w) 802(w) 730(m) 703(m) 640(s) 627(s) 558(m) 490(m) cm⁻¹. Raman (400 mW, 25 °C) $\tilde{\nu} = 3172(4)$ 1728(58) 1582(65) 1338(100) 1256(73) 1134(74) 1054(83) 932(63) 812(55) 708(55) 563(33) 447(43) 300(23) 181(43) 89(5) cm⁻¹. ¹H NMR ([D₆]DMSO, 25 °C): $\delta = 9.72$ (s, 1 H, NH), 8.33 (s, 4 H, NH₂), 7.14 (s, 2 H, NH₂), 3.7 (s, 2 H, H₂O). ¹³C NMR ([D₆]DMSO, 25 °C): $\delta = 155.7$ (1C, C1/C2), 154.5 (1C, C2/C1). ¹⁴N NMR ([D₆]DMSO, 25 °C): $\delta = -137$ (1N, $J = 100$ Hz, NNN), -271 (2N, $J = 290$ Hz, NNN). MS m/z (FAB⁺, xenon, 6 keV, glycerine matrix): 19.1 (4, H₃O⁺), 103.1 (100, [C₂H₇N₄O]⁺), 205.2 (30, {[C₂H₇N₄O]⁺₂ - H⁺}), 256.1 (15, [C₂H₇N₄O-matrix]⁺).

Guanylurea Azide (8b): The anhydrous compound was synthesized in quantitative yield by dehydration of **8a** (0.214 g, 1.31 mmol) at 60 °C under high vacuum (10⁻³ mbar) over 2 days.

C₂H₇N₇O (145.12 g·mol⁻¹) calcd.: C 16.55, H 4.86, N 67.56 %; found: C 16.35, H 5.01, N 67.42 %; DSC (5 °C·min⁻¹; °C): ~180 (m. p. + dec). IR (KBr): $\tilde{\nu} = 3212$ (s) 3172(s) 2117(m) 2040(s) 1725(vs) 1696(s) 1670(s) 1645(vs) 1598(s) 1531(m) 1455(s) 1397(s) 1385(m) 1357(s) 1170(m) 1112(m) 1089(m) 1054(m) 876(w) 730(m) 699(m) 625(s) 564(w) 498(w) cm⁻¹. Raman (400 mW, 25 °C) $\tilde{\nu} = 3092(3)$ 1723(43) 1585(57) 1337(100) 1259(68) 1137(81) 1057(89) 936(54) 818(42) 714(37) 607(2) 566(21) 452(37) 308(26) 254(3) 180(42) 91(3) cm⁻¹. ¹H NMR ([D₆]DMSO, 25 °C): $\delta = 9.82$ (s, 1 H, NH), 8.25 (s, 4 H, NH₂), 7.22 (s, 2 H, NH₂). ¹³C NMR ([D₆]DMSO, 25 °C): $\delta = 155.5$ (1C, C1/C2), 154.3 (1C, C2/C1). ¹⁴N NMR ([D₆]DMSO, 25 °C): $\delta = -135$ (1N, $J = 90$ Hz, NNN), -274 (2N, $J = 275$ Hz, NNN).

MS m/z (FAB⁺, xenon, 6 keV, glycerine matrix): 103.1 (100, [C₂H₇N₄O]⁺), 205.2 (24, {[C₂H₇N₄O]⁺₂ - H⁺}), 256.1 (19, [C₂H₇N₄O-matrix]⁺).

Guanylurea 5-Nitrotetrazolate (9): Anhydrous ammonium 5-nitrotetrazolate (1.028 g, 7.7 mmol) was dissolved in water (20 mL) and barium hydroxide octahydrate (1.228 g, 3.89 mmol) was added to this solution. The initially insoluble material dissolved upon heating and the reaction mixture was heated under reflux for 3 hours (evolution of ammonia gas). Solid guanylurea sulfate monohydrate (1.213 g, 3.89 mmol) was added portion-wise to the hot solution causing immediate precipitation of barium sulfate. After the mixture was heated 30 minutes under reflux, the insoluble solid was filtered through a plug of celite (previously washed with water) and the celite was washed with a small volume of hot water. The filtrate was transferred into a crystallization shell and the solvent was left to evaporate slowly yielding a cream colored powder. No further purification was necessary (1.581 g, 94 %). C₃H₇N₉O₃ (217.15 g·mol⁻¹) calcd.: C 16.59, H 3.25, N 58.05 %; found: C 16.44, H 3.18, N 57.51 %; DSC (5 °C·min⁻¹; °C): 209 (m. p. + dec). IR (KBr): $\tilde{\nu} = 3461$ (vs) 3417(s) 3368(s) 3213(s) 2993(m) 2453(w) 2170(w) 2054(w) 1741(s) 1692(vs) 1638(s) 1582(s) 1538(vs) 1447(s) 1420(s) 1319(s) 1177(m) 1120(m) 1077(m) 1060(m) 1032(m) 1022(m) 915(w) 845(m) 775(w) 765(w) 723(w) 695(m) 671(m) 558(w) 490(w) 453(w) cm⁻¹. Raman (400 mW, 25 °C) $\tilde{\nu} = 3238(1)$ 1731(3) 1691(1) 1590(2) 1541(4) 1446(9) 1422(100) 1321(4) 1171(3) 1120(2) 1064(23) 1045(19) 1032(25) 1025(21) 920(2) 845(8) 771(2) 704(3) 547(3) 435(9) 261(3) 242(4) 151(3) cm⁻¹. ¹H NMR ([D₆]DMSO, 25 °C): $\delta = 9.51$ (s, 1 H, NH), 8.21 (s, 4 H, NH₂), 7.07 (s, 2 H, NH₂). ¹³C NMR ([D₆]DMSO, 25 °C): $\delta = 168.8$ (1C, C_{ring}), 155.6 (1C, C1/C2), 154.7 (1C, C2/C1). ¹⁴N NMR ([D₆]DMSO, 25 °C): $\delta = +25$ (2N, $J = 500$ Hz, N2/3), -23 (1N, $J = 80$ Hz, NO₂), -60 (2N, $J = 415$ Hz, N1/4). m/z (FAB⁺, xenon, 6 keV, *m*-NBA matrix) 114.0 (100, [N₄C-NO₂]⁻); MS m/z (FAB⁺, xenon, 6 keV, glycerine matrix): 103.1 (100, [C₂H₇N₄O]⁺), 205.2 (12, {[C₂H₇N₄O]⁺₂ - H⁺}), 256.1 (30, [C₂H₇N₄O-matrix]⁺).

Guanylurea 5-Aminotetrazolate (10): 5-Amino 1*H*-tetrazole (1.018 g, 11.61 mmol) and barium hydroxide octahydrate (1.831 g, 5.80 mmol) were suspended in water (25 mL). The reaction mixture was heated under reflux for two hours forming a clear solution and afterwards, guanylurea sulfate monohydrate (1.809 g, 5.80 mmol) was added causing the precipitation of barium sulfate. After the mixture was heated 15 min. under reflux, the solid was filtered through celite and the filtrate was rotavaporated to dryness yielding the crude product, which could be recrystallized from water/ethanol (1.815 g, 83 %). Slow evaporation of a saturated solution of the compound in methanol rendered X-ray quality single crystals. C₃H₉N₉O (187.16 g·mol⁻¹) calcd.: C 19.25, H 4.85, N 67.35 %; found: C 19.09, H 4.92, N 67.01 %; DSC (5 °C·min⁻¹; °C): 152 (m. p.) ~240 (dec). IR (KBr): $\tilde{\nu} = 3455$ (s) 3415(s) 3363(s) 3291(s) 3193(m) 2894(m) 2700(m) 2165(w) 1736(s) 1701(vs) 1603(s) 1522(s) 1481(m) 1442(m) 1431(m) 1331(m) 1222(m) 1154(w) 1109(m) 1070(m) 1018(w) 924(w) 887(w) 825(w) 774(m) 754(m) 699(m) 581(m) 566(m) 485(m) cm⁻¹. Raman (400 mW, 25 °C) $\tilde{\nu} = 3164$ (2) 1714(5) 1595(8) 1523(15) 1433(7) 1351(5) 1224(20) 1126(9) 1074(34) 1018(5) 926(13) 745(13) 697(13) 574(6) 445(25) 421(11) 348(7) 264(8) 205(7) 182(8) 100(2) 83(1) cm⁻¹. ¹H NMR ([D₆]DMSO, 25 °C) $\delta = 9.87$ (s, 1 H, NH), 8.33 (s, 4 H, NH₂), 7.47 (s, 2 H, NH₂), 6.17 (s, 2 H, NH_{2(A1)}). ¹³C NMR ([D₆]DMSO, 25 °C): $\delta = 157.6$ (1C, C_{ring}), 155.6 (1C, C1/C2), 154.4 (1C, C2/C1). MS m/z (FAB⁺, xenon, 6 keV, *m*-NBA matrix) 84.1 (35, [N₄C-NH₂]⁻), 237.1 (33, [N₄C-NH₂-matrix]⁻) 390.2 (15, [N₄C-NH₂-matrix]⁻); m/z (FAB⁺, xenon, 6 keV, glycerine matrix): 103.1 (88, [C₂H₇N₄O]⁺), 205.2 (6, {[C₂H₇N₄O]⁺₂ - H⁺}), 256.1 (19, [C₂H₇N₄O-matrix]⁺).

Guanlylurea Picrate (11): Compound **4** (1.150 g, 8.3 mmol) was dissolved in water (50 mL) in a 100 mL round-bottomed flask. Neat picric acid (1.900 g, 8.3 mmol) was added portion wise at room temperature causing precipitation of a yellow precipitate. The reaction mixture was heated to reflux for 1.5 hours. After cooling, the solid was filtered and left to air-dry yielding pure **11** (2.261 g, 82 %). $C_8H_9N_7O_8$ (331.05 g·mol⁻¹) calcd.: C 29.00, H 2.74, N 29.60 %; found: C 29.01, H 2.66, N 29.46 %; DSC (5 °C·min⁻¹; °C): 253 (m. p. + dec). **IR** (KBr): $\tilde{\nu}$ = 3434 (vw) 3397(w) 3376(w) 3167(w) 1726(m) 1693(m) 1651(w) 1608(m) 1592(m) 1563(m) 1547(m) 1510(m) 1486(m) 1446(w) 1430(m) 1363(m) 1353(m) 1320(s) 1267(s) 1164(m) 1132(m) 1080(s) 943(w) 919(m) 840(vw) 822(vw) 785(m) 743(m) 711(s) 704(s) 612(vs) 567(s) cm⁻¹. **Raman** (400 mW, 25 °C) $\tilde{\nu}$ = 1612(9) 1567(19) 1550(27) 1491(13) 1430(8) 1367(44) 1343(90) 1316(100) 1302(83) 1275(46) 1167(20) 1135(9) 1084(20) 945(21) 925(16) 826(61) 790(10) 714(15) 543(11) 461(18) 426(12) 367(12) 339(21) 292(12) 194(10) cm⁻¹. **¹H NMR** ([D₆]DMSO, 25 °C): δ = 9.56 (s, 1 H, NH), 8.57 (s, 2 H, Ar-H), 7.99 (s, 4 H, NH₂), 7.14 (s, 2 H, NH₂). **¹³C NMR** ([D₆]DMSO, 25 °C): δ = 160.8 (2C, C–NO₂), 155.4 (1C, C₁/C₂), 154.4 (1C, C₂/C₁), 141.8 (1C, CO), 125.2 (2C, CH), 124.3 (1C, C–NO₂). **¹⁴N NMR** ([D₆]DMSO, 25 °C): δ = –12 (3N, *J* = 300 Hz, NO₂). **MS** *m/z* (FAB⁻, xenon, 6 keV, glycerine matrix): 227.9 (8, [C₆H₂N₃O₇]⁻), *m/z* (FAB⁺, xenon, 6 keV, glycerine matrix): 103.1 (14, [C₂H₇N₄O]⁺), 205.1 (1, {[C₂H₇N₄O]⁺₂ – H⁺}), 241.1 (3, {[C₂H₇N₄OCl]⁺·[C₂H₇N₄O]⁺}).

Guanlylurea 5,5'-Azotetrazolate Hemihydrate (12a): Sodium 5,5'-azotetrazolate pentahydrate (2.502 g, 8.34 mmol) [48] was dissolved in boiling water (25 mL) and a solution of guanlylurea chloride (2.420 g, 16.68 mmol) in boiling water (25 mL) was added to this mixture. A yellow solid precipitated and the reaction mixture was heated under reflux for 1 hour. Afterwards, it was left to cool slowly. The yellow highly insoluble powder was filtered, washed with water and left to air-dry (2.575 g, 81 %). Elemental analysis showed the presence of half a molecule of water and repeated recrystallization from water did not vary this result. $C_6H_{15}N_{18}O_{2.5}$ (379.12 g·mol⁻¹) calcd.: C 19.00, H 3.99, N 66.46 %; found: C 18.98, H 3.95, N 66.28 %; DSC (5 °C·min⁻¹; °C): 213 (dec), 240 (dec). **IR** (KBr): $\tilde{\nu}$ = 3450 (s) 3400(vs) 3318(vs) 3203(vs) 2798(s) 2215(w) 1720(vs) 1641(vs) 1595(vs) 1529(m) 1467(m) 1448(m) 1397(s) 1356(s) 1195(m) 1176(m) 1160(m) 1135(m) 1088(m) 1080(m) 1030(m) 930(w) 841(m) 794(w) 770(m) 737(s) 702(m) 614(s) 571(m) 556(s) 446(m) 428(w) cm⁻¹. **Raman** (400 mW, 25 °C) $\tilde{\nu}$ = 1480(42) 1420(32) 1379(100) 1309(3) 1193(4) 1093(10) 1076(6) 1054(41) 1033(16) 976(6) 923(8) 448(6) 377(4) 168(4) cm⁻¹. **¹H NMR** ([D₆]DMSO, 25 °C): δ = 9.3 (s, 1 H, NH), 8.0 (s, 4 H, NH₂), 7.1 (s, 2 H, NH₂), 4.0 (s, 1 H, H₂O). **¹³C NMR** ([D₆]DMSO, 25 °C): δ = 173.0 (2C, C_{ring}), 155.7 (1C, C₁/C₂), 154.5 (1C, C₂/C₁). **MS** *m/z* (FAB⁻, xenon, 6 keV, glycerine matrix): 168.0 (100, [C₂HN₁₀]⁻), 331.0 (5, [C₂H₂N₁₀·C₂HN₁₀]⁻); *m/z* (FAB⁺, xenon, 6 keV, glycerine matrix): 103.0 (10, [C₆H₂N₃O₇]⁻), 205.0 (4, {[C₂H₇N₄O]⁺₂ – H⁺}).

Guanlylurea 5,5'-Azotetrazolate (12b): Method 1. Sodium 5,5'-azotetrazolate pentahydrate (0.951 g, 3.17 mmol) [48] was dissolved in hot water (10 mL) (~70 °C) and a solution of guanlylurea chloride (0.920 g, 6.34 mmol) in hot water (10 mL) was added. Immediate precipitation of a yellow solid was observed and the reaction mixture was shortly heated to reflux. After this time, the insoluble solid was filtered hot, washed with cold water, acetone and dried under vacuum (1.003 g, 85 %). No further purification was necessary.

Method 2. Alternatively, the hemihydrate compound (**12a**) could be dehydrated quantitatively by heating at 70 °C for 2 days. $C_6H_{14}N_{18}O_2$ (370.15 g·mol⁻¹) calcd.: C 19.45, H 3.81, N 68.09 %; found: C 19.39,

H 3.91, N 67.19 %; DSC (5 °C·min⁻¹; °C): 199 (dec), 240 (dec). **IR** (KBr): $\tilde{\nu}$ = 3446 (vw) 3397(w) 3313(m) 3194(m) 2789(w) 2213(vw) 1718(vs) 1684(s) 1639(s) 1586(s) 1528(w) 1465(w) 1445(w) 1396(s) 1353(s) 1194(m) 1128(m) 1088(m) 1040(w) 1026(s) 930(w) 832(s) 768(s) 738(s) 701(s) cm⁻¹. **Raman** (400 mW, 25 °C) $\tilde{\nu}$ = 1481(43) 1420(31) 1379(100) 1192(4) 1093(11) 1054(38) 1032(15) 921(8) 703(2) 451(4) 162(2) cm⁻¹. **¹H NMR** ([D₆]DMSO, 25 °C): δ = 9.4 (s, 1 H, NH), 8.1 (s, 4 H, NH₂), 7.1 (s, 2 H, NH₂). **¹³C NMR** ([D₆]DMSO, 25 °C): δ = 172.7 (2C, C_{ring}), 155.9 (1C, C₁/C₂), 155.4 (1C, C₂/C₁). **MS** *m/z* (FAB⁻, xenon, 6 keV, glycerine matrix): 168.0 (100, [C₂HN₁₀]⁻), 331.0 (7, [C₂H₂N₁₀·C₂HN₁₀]⁻); *m/z* (FAB⁺, xenon, 6 keV, glycerine matrix): 103.0 (8, [C₆H₂N₃O₇]⁻), 205.0 (2, {[C₂H₇N₄O]⁺₂ – H⁺}).

Supporting Information (see footnote on the first page of this article): Calculated IR and Raman frequencies, X-ray, electronic energies and energetic tables and a description of the general method used here.

Acknowledgement

Financial support of this work by the *Ludwig-Maximilian University of Munich* (LMU), the *Fonds der Chemischen Industrie* (FCI), the European Research Office (ERO) of the *U. S. Army Research Laboratory* (ARL) and *ARDEC* (Armament Research, Development and Engineering Center) under contract nos. N 62558-05-C-0027, R&D 1284-CH-01, R&D 1285-CH-01, 9939-AN-01 & W911NF-07-1-0569 and the *Bundeswehr Research Institute for Materials, Explosives, Fuels and Lubricants* (WIWEB) under contract nos. E/E210/4D004/X5143 & E/E210/7D002/4F088 is gratefully acknowledged. The authors acknowledge collaborations *Dr. M. Krupka* (OZM Research, Czech Republic) in the development of new testing and evaluation methods for energetic materials and with *Dr. M. Suscesca* (Brodarski Institute, Croatia) in the development of new computational codes to predict the detonation parameters of high-nitrogen explosives. We are indebted to and thank *Dr. Betsy M. Rice* (ARL, Aberdeen, Proving Ground, MD) for many helpful and inspired discussions and support of our work.

References

- [1] a) S. Radhakrishnan, M. B. Talawar, S. Venugopalan, V. L. Narasimhan, *J. Hazard. Mater.* **2008**, *152*, 1317–1324; b) T. M. Klapötke, C. Miró Sabaté, *Chem. Mater.* **2008**, *20*, 1750–1763; c) M. Göbel, T. M. Klapötke, *Acta Crystallogr.* **2008**, *C64(2)*, o58–o60; d) T. M. Klapötke, J. Stierstorfer, *Helvet. Chim. Acta* **2007**, *90*, 2132–2150; e) S. Xu, S. Yang, *HanNeng CaiLiao*, **2006**, *14*, 377–380; f) T. M. Klapötke, C. Miró Sabaté, *Z. Anorg. Allg. Chem.* **2007**, *633*, 2671–2677; g) C. Darwich, K. Karagiosoff, T. M. Klapötke, C. Miró Sabaté, *Z. Anorg. Allg. Chem.* **2008**, *634*, 61–68; h) K. Karagiosoff, T. M. Klapötke, P. Mayer, C. Miró Sabaté, A. Penger, J. M. Welch, *Inorg. Chem.* **2008**, *47*, 1007–1019; i) T. M. Klapötke, C. Miró Sabaté, M. Rusan, *Z. Anorg. Allg. Chem.* **2008**, *634*, 688–695; j) T. M. Klapötke, C. Miró Sabaté, J. M. Welch, *Z. Anorg. Allg. Chem.* **2008**, *634*, 857–866.
- [2] a) Z. Zeng, H. Gao, B. Twamley, J. M. Shreeve, *J. Mater. Chem.* **2007**, *17*, 3819–3826; b) H. Xue, H. Gao, B. Twamley, J. M. Shreeve, *Chem. Mater.* **2007**, *19*, 1731–1739; c) H. Gao, C. Ye, O. D. Gupta, J. C. Xiao, M. A. Hiskey, B. Twamley, J. M. Shreeve, *Chem. Eur. J.* **2007**, *13*, 3853–3860; d) Y. Gao, B. Twamley, J. M. Shreeve, *Chem. Eur. J.* **2006**, *12*, 9010–9018.
- [3] a) R. P. Singh, R. D. Verma, D. T. Meshri, J. M. Shreeve, *Angew. Chem. Int. Ed.* **2006**, *45*, 3584–3601; b) H. Xue, B. Twamley, J. M. Shreeve, *Eur. J. Inorg. Chem.* **2006**, 2959–2965; c) H. Gao, R. Wang, B. Twamley, M. A. Hiskey, J. M. Shreeve,

- Chem. Commun.* **2006**, 4007–4009; d) R. Wang, H. Gao, C. Ye, B. Twamley, J. M. Shreeve, *Inorg. Chem.* **2007**, *46*, 932–938; e) H. Gao, C. Ye, O. D. Gupta, J. C. Xiao, M. A. Hiskey, B. Twamley, J. M. Shreeve, *Chem. Eur. J.* **2007**, *13*, 3853–3860; f) Y. Huang, H. Gao, B. Twamley, J. M. Shreeve, *Eur. J. Inorg. Chem.* **2007**, 2025–2030; g) C. Ye, H. Gao, B. Twamley, J. M. Shreeve, *New J. Chem.* **2008**, *32*, 317–322; h) H. Gao, Z. Zeng, B. Twamley, J. M. Shreeve, *Chem. Eur. J.* **2008**, *14*, 1282–1290.
- [4] a) J. Geith, G. Holl, T. M. Klapötke, J. J. Weigand, *Combust. Flame* **2004**, *139*, 358–366; b) J. Geith, T. M. Klapötke, J. Weigand, G. Holl, *Propell. Explos. Pyrotech.* **2004**, *29*, 3–8.
- [5] L. A. Deshusses, J. Deshusses, *Helvet. Chim. Acta* **1933**, *16*, 783–792.
- [6] G. H. Foster, D. W. Jayne, *US* 2,277,823, **1942**.
- [7] K. Szabo, A. H. Freiberg, *US* 3,479,437, **1969**.
- [8] J. J. Hlavka, P. Bitha, Y. I. Lin, *US* 4,544,759, **1985**.
- [9] a) W. T. A. Harrison, *Sol. Sta. Sci.* **2006**, *8*, 371–378; b) I. V. Medrish, E. V. Peresypkina, A. V. Virovets, L. B. Serezhkina, *Russ. J. Coord. Chem.* **2006**, *32*, 910–914; c) P. Bhattacharjee, M. Prasad, P. Kumari, *Orient. J. Chem.* **1998**, *14*, 259–265.
- [10] a) R. K. Ray, G. B. Kauffman, *Polyhedron* **1994**, *13*, 2591–2598; b) R. K. Ray, M. K. Bandyopadhyay, G. B. Kauffman, *Polyhedron* **1989**, *8*, 757–762; c) C. R. Saha, S. K. Hota, *Ind. J. Chem.* **1986**, *25A*, 340–344; d) A. Syamal, P. K. Mandal, S. K. Verma, *Transition. Met. Chem.* **1978**, *3*, 288–291; e) C. R. Saha, *J. Inorg. Nucl. Chem.* **1976**, *38*, 1635–1640; f) D. Sen, C. Saha, *J. Chem. Soc., Dalton Trans.* **1976**, *9*, 776–779.
- [11] a) Y. Guo, H. Gao, B. Twamley, J. M. Shreeve, *Adv. Mater.* **2007**, *19*, 2884–2888. b) A. Hammerl, M. A. Hiskey, G. Holl, T. M. Klapötke, K. Polborn, J. Stierstorfer, J. J. Weigand, *Chem. Mater.* **2005**, *17*, 3784–3793. c) T. M. Klapötke, P. Mayer, C. Miró Sabaté, J. M. Welch, N. Wiegand, *Inorg. Chem.* **2008**, *47*, 6014–6027.
- [12] a) A. Langlet, *WO* 9,855,428, **1998**; b) N. Latypov, A. Langlet, *WO* 9,946,202, **1999**; c) P. Sjöberg, *WO* 0,040,523, **2000**; d) C. Voerde, H. Skifs, *WO* 0,070,823, **2005**.
- [13] H. Östmark, U. Bemm, H. Bergman, A. Langlet, *Thermoch. Acta* **2002**, *384*, 253–259.
- [14] a) U. Bemm, H. Ostmark, *Acta Crystallog.* **1998**, *C54*, 1997–1999; b) N. V. Latypov, J. Bergman, A. Langlet, U. Wellmar, U. Bemm, *Tetrahedron* **1998**, *54*, 11525–11536; c) T. M. Klapötke, *Moderne Anorganische Chemie*, 2nd ed., Walter de Gruyter, Berlin/New York, Germany/USA, **2003**; d) J. Evers, T. M. Klapötke, P. Mayer, G. Oehlinger, J. Welch, *Inorg. Chem.* **2006**, *45*, 4996–5007.
- [15] a) H. Xue, J. M. Shreeve, *Adv. Mater.* **2005**, *17*, 2142; b) H. Xue, B. Twamley, J. M. Shreeve, *Inorg. Chem.* **2005**, *44*, 7009.
- [16] M. Scoptoni, E. Polo, V. Bertolasi, V. Carassiti, G. Bertelli, *J. Chem. Soc., Perkin Trans. Part 1*, **1991**, *10*, 1619–1624.
- [17] R. Andreasch, *Monat. Chem.* **1927**, *48*, 145–154.
- [18] T. Ooshima, S. Kuroda, Y. Nosaka, *JP* 45,040,898, **1970**.
- [19] T. M. Klapötke, C. Miró Sabaté, *Heteroat. Chem.* **2008**, *19*, 301–306.
- [20] M. J. Frisch, G. W. Trucks, H. B. Schlegel, G. E. Scuseria, M. A. Robb, J. R. Cheeseman, J. A. Montgomery Jr., T. Vreven, K. N. Kudin, J. C. Burant, J. M. Millam, S. S. Iyengar, J. Tomasi, V. Barone, B. Mennucci, M. Cossi, G. Scalmani, N. Rega, G. A. Petersson, H. Nakatsuji, M. Hada, M. Ehara, K. Toyota, R. Fukuda, J. Hasegawa, M. Ishida, T. Nakajima, Y. Honda, O. Kitao, H. Nakai, M. Klene, X. Li, J. E. Knox, H. P. Hratchian, J. B. Cross, C. Adamo, J. Jaramillo, R. Gomperts, R. E. Stratmann, O. Yazyev, A. J. Austin, R. Cammi, C. Pomelli, J. W. Ochterski, P. Y. Ayala, K. Morokuma, G. A. Voth, P. Salvador, J. J. Dannenberg, V. G. Zakrzewski, S. Dapprich, A. D. Daniels, M. C. Strain, O. Farkas, D. K. Malick, A. D. Rabuck, K. Raghavachari, J. B. Foresman, J. V. Ortiz, Q. Cui, A. G. Baboul, S. Clifford, J. Cioslowski, B. B. Stefanov, G. Liu, A. Liashenko, P. Piskorz, I. Komaromi, R. L. Martin, D. J. Fox, T. Keith, M. A. Al-Laham, C. Y. Peng, A. Nanayakkara, M. Challacombe, P. M. W. Gill, B. Johnson, W. Chen, M. W. Wong, C. Gonzalez, J. A. Pople, *Gaussian G03W*, Gaussian 03, Revision A.1, Gaussian Inc., Pittsburgh PA, **2003**.
- [21] J. A. Pople, R. Seeger, R. Krishnan, *Int. J. Quantum Chem. Symp.* **1977**, *11*, 149–163.
- [22] A. P. Scott, L. Radom, *J. Phys. Chem.* **1996**, *100*, 16502–16513.
- [23] A. K. Rick, T. H. Dunning, J. H. Robert, *J. Chem. Phys.* **1992**, *96*, 6796–6806.
- [24] A. P. Kirk, E. W. David, T. H. Dunning, *J. Chem. Phys.* **1994**, *100*, 7410–7415.
- [25] a) T. M. Klapötke, C. Miró Sabaté, J. Welch, *Dalton Trans.* **2008**, 6372–6380; b) T. M. Klapötke, C. Miró Sabaté, J. Welch, *Eur. J. Inorg. Chem.* **2009**, 769–776; c) T. M. Klapötke, C. Miró Sabaté, *Z. Anorg. Allg. Chem.* **2009**, DOI: 10.1002/zaac.200801357; d) T. M. Klapötke, C. Miró Sabaté, *Z. Anorg. Allg. Chem.* **2008**, *634*, 1017–1024; e) T. M. Klapötke, C. Miró Sabaté, *Eur. J. Inorg. Chem.* **2008**, *34*, 5350–5366; f) N. B. Colthup, L. H. Daly, S. E. Wiberley, *Introduction to Infrared and Raman Spectroscopy*, Academic Press, Boston, USA, **1990**.
- [26] *CrysAlis CCD*, version 1.171.27p5 beta, Oxford Diffraction Ltd.
- [27] *CrysAlis RED*, version 1.171.27p5 beta, Oxford Diffraction Ltd.
- [28] a) A. Altomare, G. Cascarano, C. Giacovazzo, A. Guagliardi, *J. Appl. Crystallogr.* **1993**, *26*, 343; b) A. Altomare, M. C. Burla, M. Camalli, G. L. Cascarano, C. Giacovazzo, A. Guagliardi, A. G. Moliterni, G. Polidori, R. Spagna, *J. Appl. Crystallogr.* **1999**, *32*, 115–119.
- [29] G. M. Sheldrick, *SHELX-92*, Program for Crystal Structure Solution, Institut für Anorganische Chemie der Universität Göttingen, Germany, **1994**.
- [30] G. M. Sheldrick, *SHELX-97*, Program for Crystal Structure Solution, Institut für Anorganische Chemie der Universität Göttingen, Germany, **1997**.
- [31] L. J. Farrugia, *J. Appl. Crystallogr.* **1999**, *32*, 837.
- [32] A. L. Spek, *PLATON*, A Multipurpose Crystallographic Tool, Utrecht, The Netherlands, **1999**.
- [33] CCDC-numbers -737952 (**4**), -665842 (**7**), -737953 (**8a**) and -737954 (**10**) contain the supplementary crystallographic data for this paper. These data can be obtained free of charge from The Cambridge Crystallographic Data Centre via www.ccdc.cam.ac.uk/data_request/cif.
- [34] A. F. Hollemann, E. Wieberg, N. Wieberg, *Lehrbuch der Anorganischen Chemie*, 101th ed., Walter de Gruyter, Berlin, **1995**.
- [35] A. Bondi, *J. Phys. Chem.* **1964**, *68*, 441–451.
- [36] a) J. Bernstein, R. E. Davis, L. Shimoni, N. L. Chang, *Angew. Chem. Int. Ed. Engl.* **1995**, *34*, 1555–1573; b) W. D. S. Motherwell, G. P. Shields, F. H. Allen, *Acta Crystallogr., Sect. B* **2000**, *56*, 466–473; c) W. D. S. Motherwell, G. P. Shields, F. H. Allen, *Acta Crystallogr., Sect. B* **1999**, *55*, 1044–1056; d) <http://www.ccdc.cam.ac.uk/support/documentation/rpluto/TOC.html>
- [37] a) T. M. Klapötke, K. Karaghiosoff, P. Mayer, A. Penger, J. M. Welch, *Propell. Explos. Pyrotech.* **2006**, *31*, 188–195; b) V. Ernst, T. M. Klapötke, J. Stierstorfer, *Z. Anorg. Allg. Chem.* **2007**, *633*, 879–887.
- [38] a) M. Göbel, T. M. Klapötke, *Z. Anorg. Allg. Chem.* **2007**, *633*, 1006–1017; b) C. Darwich, T. M. Klapötke, C. Miró Sabaté, *Chem. Eur. J.* **2008**, *14*, 5756–5771; c) T. M. Klapötke, C. Miró Sabaté, *Chem. Mater.* **2008**, *20*, 3629–3637.
- [39] J. Köhler, R. Meyer, *Explosivstoffe*, 7th ed., Wiley-VCH, Weinheim, Germany, **1991**.
- [40] a) H. D. B. Jenkins, D. Tudela, L. Glasser, *Inorg. Chem.* **2002**, *41*, 2364–2367; b) H. D. B. Jenkins, H. K. Roobottom, J. Passmore, L. Glasser, *Inorg. Chem.* **1999**, *38*, 3609–3620.
- [41] H. Gao, C. Ye, C. M. Piekarski, J. M. Shreeve, *J. Phys. Chem.* **2007**, *C111*, 10718–10731.
- [42] M. Suceca, *Propell. Explos. Pyrotech.* **1991**, *16*, 197–202.
- [43] J. Akhavan, *The Chemistry of Explosives*, 2nd ed., RSC Paperbacks: Cambridge, UK, **2004**.
- [44] H. Gao, Z. Zeng, B. Twamley, J. M. Shreeve, *Chem. Eur. J.* **2008**, *14*, 1282–1290.

- [45] *UN Recommendations on the Transport of Dangerous Goods, Manual of Tests and Criteria.*, 4th ed.; United Nations: New York, **2003**.
- [46] <http://www.systag.ch>.
- [47] *ICT-Thermodynamic Code, Version 1.0*, Fraunhofer-Institut für Chemische Technologie, Pfingztal, Germany, **1988–2000**; R. Webb, M. van Rooijen, *Proceedings of the 29th International Pyrotechnics Seminar*, Westminster, CO, **2002**.
- [48] a) J. Thiele, *Justus Liebigs Ann. Chem.* **1892**, 270, 54–63; b) J. Thiele, J. T. Marais, *Justus Liebigs Ann. Chem.* **1893**, 273, 144–160; c) J. Thiele, *Ber. Dtsch. Chem. Ges.* **1893**, 26, 2645–2646; d) J. Thiele, *Justus Liebigs Ann. Chem.* **1898**, 303, 57–75.

Received: July 7, 2009
Published Online: September 17, 2009